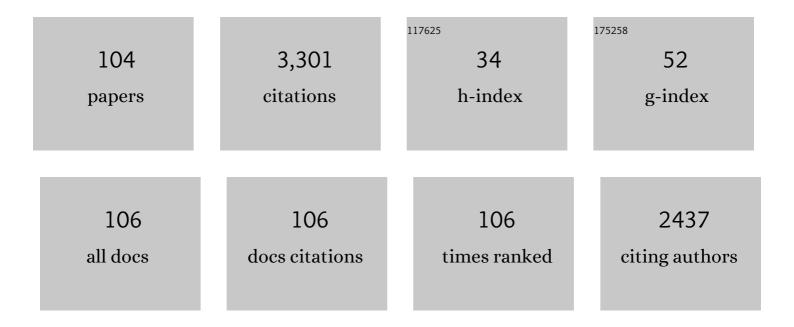
Cheng-Xin Li

List of Publications by Year in descending order

Source: https://exaly.com/author-pdf/1053646/publications.pdf Version: 2024-02-01



#	Article	IF	CITATIONS
1	Effect of <scp><scp>TGO</scp></scp> Thickness on Thermal Cyclic Lifetime and Failure Mode of Plasma‧prayed <scp><scp>TBC</scp></scp> s. Journal of the American Ceramic Society, 2014, 97, 1226-1232.	3.8	157
2	Material nucleation/growth competition tuning towards highly reproducible planar perovskite solar cells with efficiency exceeding 20%. Journal of Materials Chemistry A, 2017, 5, 6840-6848.	10.3	149
3	Large-area high-efficiency perovskite solar cells based on perovskite films dried by the multi-flow air knife method in air. Journal of Materials Chemistry A, 2017, 5, 1548-1557.	10.3	115
4	Influence of TGO Composition on the Thermal Shock Lifetime of Thermal Barrier Coatings with Cold-sprayed MCrAlY Bond Coat. Journal of Thermal Spray Technology, 2010, 19, 168-177.	3.1	98
5	Characterization of Nanostructured WC-Co Deposited by Cold Spraying. Journal of Thermal Spray Technology, 2007, 16, 1011-1020.	3.1	97
6	Cobalt-substituted SrTi _{0.3} Fe _{0.7} O _{3â^î^} : a stable high-performance oxygen electrode material for intermediate-temperature solid oxide electrochemical cells. Energy and Environmental Science, 2018, 11, 1870-1879.	30.8	93
7	Preparation of flexible perovskite solar cells by a gas pump drying method on a plastic substrate. Journal of Materials Chemistry A, 2016, 4, 3704-3710.	10.3	87
8	Development of Particle Interface Bonding in Thermal Spray Coatings: A Review. Journal of Thermal Spray Technology, 2013, 22, 192-206.	3.1	86
9	Low-temperature SnO ₂ -modified TiO ₂ yields record efficiency for normal planar perovskite solar modules. Journal of Materials Chemistry A, 2018, 6, 10233-10242.	10.3	75
10	Relationship Between Lamellar Structure and Elastic Modulus of Thermally Sprayed Thermal Barrier Coatings with Intra-splat Cracks. Journal of Thermal Spray Technology, 2015, 24, 1355-1367.	3.1	74
11	Sinteringâ€induced delamination of thermal barrier coatings by gradient thermal cyclic test. Journal of the American Ceramic Society, 2017, 100, 1820-1830.	3.8	74
12	Recent progress of perovskite-based electrolyte materials for solid oxide fuel cells and performance optimizing strategies for energy storage applications. Materials Research Bulletin, 2022, 146, 111612.	5.2	74
13	Microstructural and Mechanical Property Evolutions of Plasma-Sprayed YSZ Coating During High-Temperature Exposure: Comparison Study Between 8YSZ and 20YSZ. Journal of Thermal Spray Technology, 2013, 22, 1294-1302.	3.1	71
14	Influence of Powder Porous Structure on the Deposition Behavior of Cold-Sprayed WC-12Co Coatings. Journal of Thermal Spray Technology, 2008, 17, 742-749.	3.1	68
15	Optimization of In-Situ Shot-Peening-Assisted Cold Spraying Parameters for Full Corrosion Protection of Mg Alloy by Fully Dense Al-Based Alloy Coating. Journal of Thermal Spray Technology, 2017, 26, 173-183.	3.1	65
16	Evolution of Lamellar Interface Cracks During Isothermal Cyclic Test of Plasma-Sprayed 8YSZ Coating with a Columnar-Structured YSZ Interlayer. Journal of Thermal Spray Technology, 2013, 22, 1374-1382.	3.1	64
17	Influence of Microstructure on the Ionic Conductivity of Plasma-Sprayed Yttria-Stabilized Zirconia Deposits. Journal of the American Ceramic Society, 2008, 91, 3931-3936.	3.8	59
18	High-Temperature Erosion of HVOF Sprayed Cr3C2-NiCr Coating and Mild Steel for Boiler Tubes. Journal of Thermal Spray Technology, 2008, 17, 782-787.	3.1	58

#	Article	IF	CITATIONS
19	Cost effective perovskite solar cells with a high efficiency and open-circuit voltage based on a perovskite-friendly carbon electrode. Journal of Materials Chemistry A, 2018, 6, 8271-8279.	10.3	57
20	Microstructural Characterization of Cold-Sprayed Nanostructured FeAl Intermetallic Compound Coating and its Ball-Milled Feedstock Powders. Journal of Thermal Spray Technology, 2007, 16, 669-676.	3.1	55
21	Performance evaluation of highly active and novel La0.7Sr0.3Ti0.1Fe0.6Ni0.3O3-Î [^] material both as cathode and anode for intermediate-temperature symmetrical solid oxide fuel cell. Journal of Power Sources, 2020, 472, 228498.	7.8	54
22	Atmospheric plasma-sprayed La _{0.8} Sr _{0.2} Ga _{0.8} Mg _{0.2} O ₃ electrolyte membranes for intermediate-temperature solid oxide fuel cells. Journal of Materials Chemistry A, 2015, 3, 7535-7553.	10.3	50
23	The Correlation of the TBC Lifetimes in Burner Cycling Test with Thermal Gradient and Furnace Isothermal Cycling Test by TGO Effects. Journal of Thermal Spray Technology, 2017, 26, 378-387.	3.1	50
24	Morphology and Size Evolution of Interlamellar Two-Dimensional Pores in Plasma-Sprayed La2Zr2O7 Coatings During Thermal Exposure at 1300°C. Journal of Thermal Spray Technology, 2015, 24, 739-748.	3.1	48
25	Mechanical property and wear performance dependence on processing condition for cold-sprayed WC-(nanoWC-Co). Applied Surface Science, 2015, 332, 80-88.	6.1	47
26	Formation of NiAl Intermetallic Compound by Cold Spraying of Ball-Milled Ni/Al Alloy Powder Through Postannealing Treatment. Journal of Thermal Spray Technology, 2008, 17, 715-720.	3.1	45
27	A Novel Plasma-Sprayed Durable Thermal Barrier Coating with a Well-Bonded YSZ Interlayer Between Porous YSZ and Bond Coat. Journal of Thermal Spray Technology, 2012, 21, 383-390.	3.1	45
28	Modeling Thermal Conductivity of Thermally Sprayed Coatings with Intrasplat Cracks. Journal of Thermal Spray Technology, 2013, 22, 1328-1336.	3.1	45
29	Hierarchical Formation of Intrasplat Cracks in Thermal Spray Ceramic Coatings. Journal of Thermal Spray Technology, 2016, 25, 959-970.	3.1	41
30	Improvement of Adhesion and Cohesion in Plasma-Sprayed Ceramic Coatings by Heterogeneous Modification of Nonbonded Lamellar Interface Using High Strength Adhesive Infiltration. Journal of Thermal Spray Technology, 2013, 22, 36-47.	3.1	39
31	Sintering behavior of BaCe0.7Zr0.1Y0.2O3-δ electrolyte at 1150°C with the utilization of CuO and Bi2O3 as sintering aids and its electrical performance. International Journal of Hydrogen Energy, 2022, 47, 7403-7414.	7.1	39
32	Characterization of Plasma Jet in Plasma Spray-Physical Vapor Deposition of YSZ Using a <80ÂkW Shrouded Torch Based on Optical Emission Spectroscopy. Journal of Thermal Spray Technology, 2015, 24, 1038-1045.	3.1	37
33	Isothermal Oxidation Behavior of NiCoCrAlTaY Coating Deposited by High Velocity Air-Fuel Spraying. Journal of Thermal Spray Technology, 2012, 21, 391-399.	3.1	36
34	Thermal Failure of Nanostructured Thermal Barrier Coatings with Cold-Sprayed Nanostructured NiCrAlY Bond Coat. Journal of Thermal Spray Technology, 2008, 17, 838-845.	3.1	34
35	Edge Effect on Crack Patterns in Thermally Sprayed Ceramic Splats. Journal of Thermal Spray Technology, 2017, 26, 302-314.	3.1	34
36	Examination of Substrate Surface Melting-Induced Splashing During Splat Formation in Plasma Spraying. Journal of Thermal Spray Technology, 2006, 15, 717-724.	3.1	33

#	Article	IF	CITATIONS
37	Plasma spray–physical vapor deposition toward advanced thermal barrier coatings: a review. Rare Metals, 2020, 39, 479-497.	7.1	33
38	High stability SrTi _{1â^'x} Fe _x O _{3â^´î^} electrodes for oxygen reduction and oxygen evolution reactions. Journal of Materials Chemistry A, 2019, 7, 21447-21458.	10.3	32
39	Plasma-Sprayed Thermal Barrier Coatings with Enhanced Splat Bonding for CMAS and Corrosion Protection. Journal of Thermal Spray Technology, 2016, 25, 213-221.	3.1	31
40	Healing of the Interface Between Splashed Particles and Underlying Bulk Coating and Its Influence on Isothermal Oxidation Behavior of LPPS MCrAlY Bond Coat. Journal of Thermal Spray Technology, 2015, 24, 611-621.	3.1	29
41	Characterization of Nonmelted Particles and Molten Splats in Plasma-Sprayed Al2O3 Coatings by a Combination of Scanning Electron Microscopy, X-ray Diffraction Analysis, and Confocal Raman Analysis. Journal of Thermal Spray Technology, 2013, 22, 131-137.	3.1	27
42	Formation of Lamellar Pores for Splats via Interfacial or Sub-interfacial Delamination at Chemically Bonded Region. Journal of Thermal Spray Technology, 2017, 26, 315-326.	3.1	27
43	Numerical simulation of the flow characteristics inside a novel plasma spray torch. Journal Physics D: Applied Physics, 2019, 52, 335203.	2.8	27
44	Measurement and Numerical Simulation of Particle Velocity in Cold Spraying. Journal of Thermal Spray Technology, 2006, 15, 559-562.	3.1	26
45	Thermally sprayed high-performance porous metal-supported solid oxide fuel cells with nanostructured La _{0.6} Sr _{0.4} Co _{0.2} Fe _{0.8} O _{3â^î^} cathodes. lournal of Materials Chemistry A. 2016. 4. 7461-7468.	10.3	25
46	Highly active and novel A-site deficient symmetric electrode material (Sr0.3La0.7)1â^'x (Fe0.7Ti0.3)0.9Ni0.1O3â^'l´ and its effect on electrochemical performance of SOFCs. International Journal of Hydrogen Energy, 2021, 46, 8778-8791.	7.1	25
47	Evaporation of Droplets in Plasma Spray–Physical Vapor Deposition Based on Energy Compensation Between Self-Cooling and Plasma Heat Transfer. Journal of Thermal Spray Technology, 2017, 26, 1641-1650.	3.1	24
48	Novel Method of Aluminum to Copper Bonding by Cold Spray. Journal of Thermal Spray Technology, 2018, 27, 624-640.	3.1	23
49	Understanding the Formation of Limited Interlamellar Bonding in PlasmaÂSprayed Ceramic Coatings Based on the Concept of Intrinsic Bonding Temperature. Journal of Thermal Spray Technology, 2016, 25, 1617-1630.	3.1	22
50	Effect of Spray Particle Trajectory on the Measurement Signal of Particle Parameters Based on Thermal Radiation. Journal of Thermal Spray Technology, 2003, 12, 80-94.	3.1	21
51	Deposition Behavior of Semi-Molten Spray Particles During Flame Spraying of Porous Metal Alloy. Journal of Thermal Spray Technology, 2014, 23, 991-999.	3.1	20
52	Generation of Long Laminar Plasma Jets: Experimental and Numerical Analyses. Plasma Chemistry and Plasma Processing, 2019, 39, 377-394.	2.4	20
53	The Bonding Formation during Thermal Spraying of Ceramic Coatings: A Review. Journal of Thermal Spray Technology, 2022, 31, 780-817.	3.1	20
54	Development of a Ni/Al2O3 Cermet-Supported Tubular Solid Oxide Fuel Cell Assembled with Different Functional Layers by Atmospheric Plasma-Spraying. Journal of Thermal Spray Technology, 2009, 18, 83-89.	3.1	18

#	Article	IF	CITATIONS
55	Microstructure of YSZ Coatings Deposited by PS-PVD Using 45ÂkW Shrouded Plasma Torch. Materials and Manufacturing Processes, 2016, 31, 1183-1191.	4.7	18
56	Effect of Post-spray Shot Peening Treatment on the Corrosion Behavior of NiCr-Mo Coating by Plasma Spraying of the Shell–Core–Structured Powders. Journal of Thermal Spray Technology, 2018, 27, 232-242.	3.1	17
57	Development of ScSZ Electrolyte by Very Low Pressure Plasma Spraying for High-Performance Metal-Supported SOFCs. Journal of Thermal Spray Technology, 2020, 29, 223-231.	3.1	17
58	A TEM Study of the Microstructure of Plasma-Sprayed YSZ Near Inter-splat Interfaces. Journal of Thermal Spray Technology, 2015, 24, 907-914.	3.1	16
59	Thermally Sprayed Large Tubular Solid Oxide Fuel Cells and Its Stack: Geometry Optimization, Preparation, and Performance. Journal of Thermal Spray Technology, 2017, 26, 441-455.	3.1	16
60	Advanced oxygen-electrode-supported solid oxide electrochemical cells with Sr(Ti,Fe)O _{3â^îî} -based fuel electrodes for electricity generation and hydrogen production. Journal of Materials Chemistry A, 2020, 8, 25867-25879.	10.3	16
61	Formation of Pore Structure and Its Influence on the Mass Transport Property of Vacuum Cold Sprayed TiO2 Coatings Using Strengthened Nanostructured Powder. Journal of Thermal Spray Technology, 2012, 21, 505-513.	3.1	15
62	La2NiO4+Î′ Infiltration of Plasma-Sprayed LSCF Coating for Cathode Performance Improvement. Journal of Thermal Spray Technology, 2016, 25, 392-400.	3.1	15
63	Microstructure and Transparent Super-Hydrophobic Performance of Vacuum Cold-Sprayed Al2O3 and SiO2 Aerogel Composite Coating. Journal of Thermal Spray Technology, 2018, 27, 471-482.	3.1	15
64	Enhanced Electrochemical and Tribological Properties of AZ91D Magnesium Alloy via Cold Spraying of Aluminum Alloy. Journal of Thermal Spray Technology, 2019, 28, 1739-1748.	3.1	15
65	Plasma Spraying of Dense Ceramic Coating with Fully Bonded Lamellae Through Materials Design Based on the Critical Bonding Temperature Concept. Journal of Thermal Spray Technology, 2019, 28, 53-62.	3.1	15
66	Microstructural analysis of highly active cathode material La0.7Sr0.3Ti0.15Fe0.65Ni0.2O3-δ (LSTFN) by optimizing different processing parameters. Ceramics International, 2021, 47, 10893-10904.	4.8	15
67	Recent Research Advances in Plasma Spraying of Bulk-Like Dense Metal Coatings with Metallurgically Bonded Lamellae. Journal of Thermal Spray Technology, 2022, 31, 5-27.	3.1	15
68	Microstructure and Electrochemical Behavior of a Structured Electrolyte/LSM-Cathode Interface Modified by Flame Spraying for Solid Oxide Fuel Cell Application. Journal of Thermal Spray Technology, 2010, 19, 311-316.	3.1	14
69	Effect of Dispersed TiC Content on the Microstructure and Thermal Expansion Behavior of Shrouded-Plasma-Sprayed FeAl/TiC Composite Coatings. Journal of Thermal Spray Technology, 2012, 21, 689-694.	3.1	14
70	Effect of Oxidation on the Bonding Formation of Plasma-Sprayed Stainless Steel Splats onto Stainless Steel Substrate. Journal of Thermal Spray Technology, 2017, 26, 47-59.	3.1	14
71	WC-Co Composite Coating Deposited by Cold Spraying of a Core-Shell-Structured WC-Co Powder. Journal of Thermal Spray Technology, 2015, 24, 100.	3.1	13
72	Formation of Cr2O3 Diffusion Barrier Between Cr-Contained Stainless Steel and Cold-Sprayed Ni Coatings at High Temperature. Journal of Thermal Spray Technology, 2016, 25, 526-534.	3.1	13

#	Article	IF	CITATIONS
73	Sintering behavior and electrochemical performance of A-site deficient SrxTi0.3Fe0·7O3-δ oxygen electrodes for solid oxide electrochemical cells. Ceramics International, 2021, 47, 25051-25058.	4.8	13
74	Influence of Silver Doping on Photocatalytic Activity of Liquid-Flame-Sprayed-Nanostructured TiO2 Coating. Journal of Thermal Spray Technology, 2007, 16, 881-885.	3.1	12
75	Fabrication of Porous Molybdenum by Controlling Spray Particle State. Journal of Thermal Spray Technology, 2012, 21, 1032-1045.	3.1	12
76	Effect of Phase Transformation Mechanism on the Microstructure of Cold-sprayed Ni/Al-Al2O3 Composite Coatings during Post-spray Annealing Treatment. Journal of Thermal Spray Technology, 2013, 22, 398-405.	3.1	12
77	High Heat Insulating Thermal Barrier Coating Designed with Large Two-Dimensional Inter-lamellar Pores. Journal of Thermal Spray Technology, 2016, 25, 222-230.	3.1	12
78	Optimization of Plasma-Sprayed Lanthanum Chromite Interconnector Through Powder Design and Critical Process Parameters Control. Journal of Thermal Spray Technology, 2020, 29, 212-222.	3.1	12
79	Controlling grain size in columnar YSZ coating formation by droplet filtering assisted PS-PVD processing. RSC Advances, 2015, 5, 102126-102133.	3.6	11
80	Super-Hydrophobic Surface Prepared by Lanthanide Oxide Ceramic Deposition Through PS-PVD Process. Journal of Thermal Spray Technology, 2017, 26, 398-408.	3.1	11
81	Plasma-Sprayed High-Performance (Bi2O3)0.75(Y2O3)0.25 Electrolyte for Intermediate-Temperature Solid Oxide Fuel Cells (IT-SOFCs). Journal of Thermal Spray Technology, 2021, 30, 196-204.	3.1	11
82	Fabrication of Porous Stainless Steel by Flame Spraying of Semimolten Particles. Materials and Manufacturing Processes, 2014, 29, 1253-1259.	4.7	10
83	Self-Sealing Metal-Supported SOFC Fabricated by Plasma Spraying and Its Performance under Unbalanced Gas Pressure. Journal of Thermal Spray Technology, 2020, 29, 2001-2011.	3.1	10
84	Narrow and Thin Copper Linear Pattern Deposited by Vacuum Cold Spraying and Deposition Behavior Simulation. Journal of Thermal Spray Technology, 2021, 30, 571-583.	3.1	10
85	Enhancement of Corrosion Resistance and Tribological Properties of LA43M Mg Alloy by Cold-Sprayed Aluminum Coatings Reinforced with Alumina and Carbon Nanotubes. Journal of Thermal Spray Technology, 2021, 30, 668-679.	3.1	10
86	Synthesis, Structure, Transport Properties, Electrochemical Stability Window, and Lithium Plating/Stripping of Mg and Nb Codoped Li ₇ La ₃ Zr ₂ O ₁₂ Garnet-Type Solid Electrolytes. Journal of Physical Chemistry C, 2022, 126, 7828-7840.	3.1	10
87	Performance and Stability of Plasma-Sprayed 10 × 10Âcm2 Self-sealing Metal-Supported Solid Oxide F Cells. Journal of Thermal Spray Technology, 2021, 30, 1059-1068.	uel 3.1	8
88	Preparation of bulk-like La0.8Sr0.2Ga0.8Mg0.2O3-l̂´ coatings for porous metal-supported solid oxide fuel cells via plasma spraying at increased particle temperatures. International Journal of Hydrogen Energy, 2021, 46, 32655-32664.	7.1	8
89	Ceramic Nano-particle/Substrate Interface Bonding Formation Derived from Dynamic Mechanical Force at Room Temperature: HRTEM Examination. Journal of Thermal Spray Technology, 2015, 24, 720-728.	3.1	7
90	Microstructure and Properties of Porous Ni50Cr50-Al2O3 Cermet Support for Solid Oxide Fuel Cells. Journal of Thermal Spray Technology, 2013, 22, 158-165.	3.1	6

#	Article	IF	CITATIONS
91	The Microstructure Stability of Atmospheric Plasma-Sprayed MnCo2O4 Coating Under Dual-Atmosphere (H2/Air) Exposure. Journal of Thermal Spray Technology, 2016, 25, 301-310.	3.1	5
92	Improving Erosion Resistance of Plasma-Sprayed Ceramic Coatings by Elevating the Deposition Temperature Based on the Critical Bonding Temperature. Journal of Thermal Spray Technology, 2018, 27, 25-34.	3.1	5
93	Effects of Powder Structure and Size on Gd2O3 Preferential Vaporization During Plasma Spraying of Gd2Zr2O7. Journal of Thermal Spray Technology, 2020, 29, 105-114.	3.1	5
94	Oxidation behavior and interface diffusion of porous metal supported SOFCs with all plasma sprayed functional layers in air at 650oC. International Journal of Green Energy, 2022, 19, 818-826.	3.8	4
95	Plasma-Sprayed (Bi2O3)0.705 (Er2O3)0.245 (WO3)0.05 Electrolyte for Intermediate-Temperature Solid Oxide Fuel Cells (IT-SOFCs). Journal of Thermal Spray Technology, 2022, 31, 297-306.	3.1	4
96	Study on Deposition Behavior of Less Than 5Âμm YSZ Particles in VLPPS. Journal of Thermal Spray Technology, 2020, 29, 1708-1717.	3.1	3
97	Formation of Intermetallic Compounds in a Cold-Sprayed Aluminum Coating on Magnesium Alloy Substrate after Friction Stir-Spot-Processing. Journal of Thermal Spray Technology, 2021, 30, 1464-1481.	3.1	3
98	Nonâ€destructive production of natural environmentâ€adaptive superâ€hydrophobic hierarchical ceramic surface on a steel substrate. Micro and Nano Letters, 2016, 11, 680-683.	1.3	2
99	Relationship Between Designed Three-Dimensional YSZ Electrolyte Surface Area and Performance of Solution-Precursor Plasma-Sprayed La0.8Sr0.2MnO3â~δ Cathodes. Journal of Thermal Spray Technology, 2016, 25, 1692-1699.	3.1	2
100	Suspension Plasma Sprayed Sr2Fe1.4Mo0.6O6â^î Électrodes for Solid Oxide Fuel Cells. Journal of Thermal Spray Technology, 2017, 26, 432-440.	3.1	2
101	Effect of Gas Pressure on Polarization of SOFC Cathode Prepared by Plasma Spray. Journal of Thermal Spray Technology, 2013, 22, 640-645.	3.1	1
102	Fabrication of Metal Matrix Composites via High-Speed Particle Implantation. Journal of Thermal Spray Technology, 2020, 29, 1910-1925.	3.1	1
103	Enhanced Corrosion Resistance of a Double Ceramic Composite Coating Deposited by a Novel Method on Magnesium-Lithium Alloy (LA43M) Substrates. Journal of Thermal Spray Technology, 2021, 30, 680-693.	3.1	1
104	Improving Adhesion Strength and Electrical Conductivity of Cold-Sprayed Al Deposit on Cu Substrate Through Friction-Stir-Processing. Journal of Thermal Spray Technology, 0, , 1.	3.1	0